

**JMB**Available online at [www.sciencedirect.com](http://www.sciencedirect.com) ScienceDirect

# Antibody-Induced Oligomerization and Activation of an Engineered Reporter Enzyme

Melissa L. Geddie and Ichiro Matsumura\*

Department of Biochemistry  
Center for Fundamental and  
Applied Molecular Evolution  
Emory University School of  
Medicine, Rollins Research  
Center, Room 4119  
1510 Clifton Road  
Atlanta, GA 30322, USA

Our objective is to produce a protein biosensor (or molecular switch) that is specifically activated in solution by a monoclonal antibody. Many effector-dependent enzymes have evolved in nature, but the introduction of a novel regulatory mechanism into a normally unregulated enzyme poses a difficult design problem. We used site-saturation mutagenesis and screening to generate effector-activated variants of the reporter enzyme  $\beta$ -glucuronidase (GUS). The specific activity of the purified epitope-tagged GUS variant was increased by up to ~500-fold by the addition of an equimolar concentration of a monoclonal antibody. This molecular switch is modular in design, so it can easily be re-engineered for the detection of other peptide-specific antibodies. Such antibody-activated reporters could someday enable point-of-care serological assays for the rapid detection of infectious diseases.

© 2007 Elsevier Ltd. All rights reserved.

**Keywords:** biosensor; molecular switch; high-throughput screen; induced dimerization; reporter enzyme

\*Corresponding author

## Introduction

The capacity to regulate enzymes at will would be useful for point-of-care serological diagnostics,<sup>1</sup> protein therapies,<sup>2,3</sup> and synthetic biology.<sup>4</sup> The activities of many natural proteins are regulated by posttranslational modifications or noncovalent interactions with an effector molecule. Such regulated enzymes will hereinafter be called molecular switches or protein biosensors. The textbook example of allostery is hemoglobin, a tetrameric protein that binds oxygen in a cooperative manner. The binding of O<sub>2</sub> to one subunit leads to conformational changes that increase the O<sub>2</sub> affinity of other subunits within the holoenzyme. Hemoglobin is thus a sensor and a carrier of oxygen. Allosteric proteins are fairly common in nature,<sup>5</sup> but are relatively difficult to design.

Our goal is to design molecular switches that are activated by arbitrarily designated analyte molecules. Our designs are based upon *Escherichia coli*  $\beta$ -glucuronidase (GUS) because its catalytic activity

can easily be detected with commercially available synthetic substrates. We chose a monoclonal antibody as a model analyte because an antibody-activated reporter enzyme would enable rapid serological assays. The conversion of any unregulated reporter enzyme into an antibody-activated molecular switch is a difficult protein engineering problem. GUS and other reporter enzymes (including  $\beta$ -galactosidase, alkaline phosphatase, and  $\beta$ -lactamase) are normally unregulated and, thus, are constitutively active as long as they are properly folded. The fusion of a peptide epitope to the amino or carboxy terminus of a reporter enzyme generally allows it to bind monoclonal antibodies, but these binding events rarely affect the enzyme's intrinsic catalytic activity.

First-generation protein sensors were produced by inserting peptide epitopes into permissive sites within reporter enzymes  $\beta$ -galactosidase,<sup>6</sup> alkaline phosphatase,<sup>7</sup> and  $\beta$ -lactamase.<sup>8</sup> This approach generally produces catalytically compromised enzymes that are activated up to 4-fold by antibody binding.<sup>9</sup> These switches are thought to be activated through allosteric mechanisms,<sup>10</sup> but it is difficult to predict whether the insertion of any peptide epitope within a particular position of a protein will impart the desired allosteric properties.

High-throughput screening enables the systematic evaluation of large numbers of chimeric proteins. Guntas and Ostermeier randomly inserted the gene encoding the maltose-binding protein within the

Abbreviations used: anti-HA, anti-hemagglutinin; GST, glutathione S-transferase; GUS,  $\beta$ -glucuronidase; MUG, 4-methylumbelliferyl- $\beta$ -D-glucuronide; pNP, *p*-nitrophenol; pNP-gluc, *p*-nitrophenyl  $\beta$ -D-glucuronide; X-gluc, 5-bromo-4-chloro-3-indolyl  $\beta$ -D-glucuronide.

E-mail address of the corresponding author:  
[imatsum@emory.edu](mailto:imatsum@emory.edu)

TEM-1  $\beta$ -lactamase gene.<sup>11</sup> They expressed the resulting library of maltose-binding protein- $\beta$ -lactamase chimeras in a population of *E. coli* and screened for clones that exhibit maltose-dependent  $\beta$ -lactamase activity. The enzyme activities were only modestly increased (<2-fold) by maltose,<sup>11</sup> but subsequent refinements to the approach produced  $\beta$ -lactamase variants that are significantly more responsive (>100-fold activation).<sup>12</sup> This labor-intensive library construction and high-throughput screening process would, however, have to be recapitulated to produce sensors of analytes other than maltose. Here we demonstrate a relatively simple but effective strategy for the design of antibody-activated molecular switches.

## Results

### Rationale

Our strategy was to mutate GUS, a homotetramer,<sup>13</sup> so that the resulting variant formed an inactive but soluble dimer. We were not certain which mutation combinations would accomplish this feat, so we used site-saturation mutagenesis to randomize two residues in the “short” subunit

interface (Figure 1, blue and green balls). Each monomer contains an active site close to this interface (yellow balls), so the dissociation of the tetramer into dimers would likely compromise enzyme activity. GUS mutants with diminished activity (hypomorphs) were identified in a high-throughput histological screen. The hypomorphic alleles were purified and subcloned into a vector that fused them to the glutathione S-transferase (GST) gene. The GST protein tends to dimerize proteins to which it is fused;<sup>14,15</sup> a second histological screen was used to identify GST-GUS fusions with restored GUS activity.

### GST-dependent GUS mutants

A previous study showed the mutation of particular residues in the short subunit interface of GUS improved the thermostability of the tetramer.<sup>16</sup> These results suggest subunit interactions across the short interface are essential for activity. We employed site-saturation mutagenesis to randomize two GUS codons (516 and 517) within the parental *his<sub>6</sub>-gusA-pET28a+vector* (Figure 1). Phosphorylated primers containing the degenerate NNK (where K = T or G) sequence at the two selected positions were used to PCR amplify the entire plasmid. The PCR

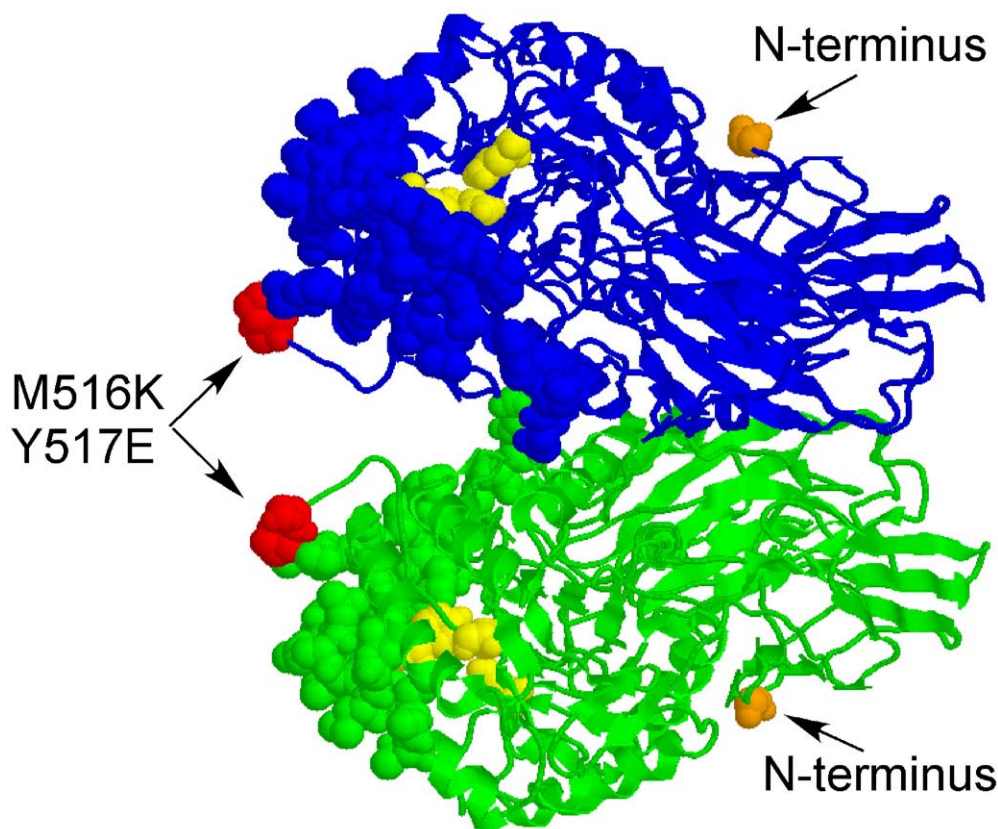


**Figure 1.** Crystal structure of human  $\beta$ -glucuronidase.<sup>13</sup>  $\beta$ -Glucuronidase is normally a homotetramer; two monomers are shown (blue and green). Residues in the “short” interface (blue and green space filling balls) normally interact with their counterparts in other subunits (not shown). Catalytic residues (yellow balls, E413, E504, Y468, *E. coli* protein numbering) are close to the short interface. The two amino acids mutated in this study are shown in red and labeled M516K/Y517E. The GST protein, HA epitope, and *myc* epitopes were separately fused to the N terminus (orange) to induce oligomerization.

product was purified, self-ligated, and used to transform *E. coli* strain DH5 $\Delta$ lac(DE3).<sup>17,18</sup>

After the transformation, ~2000 clones were grown on LB-agar plates containing kanamycin (25  $\mu$ g/ml) and chloramphenicol (34  $\mu$ g/ml). The colonies adsorbed onto nitrocellulose filters and transferred to similar plates that also contained 0.5 mM IPTG (to induce overexpression of the plasmid-borne *gusA* gene) and the histochemical GUS substrate 5-bromo-4-chloro-3-indolyl  $\beta$ -D-glucuronide (X-gluc, 80 mg/l). After being incubated overnight at 37 °C, the colonies that did not exhibit detectable GUS activity (the majority) were scraped from the filters and propagated together in liquid culture. The corresponding plasmids were isolated, and their *gusA* alleles were subcloned into expression vector pET42a+ so they were fused to the GST gene. The GST protein forms dimers<sup>19</sup> and causes proteins to which it is fused to dimerize as well.<sup>14,15</sup> The resulting library of GST-GUS variants was screened as described above for clones with restored GUS activity. Each clone with GUS activity was restreaked onto LB-kan/chl agar plates containing IPTG and X-gluc; the resulting colonies were visualized to confirm the genetic stability of their phenotypes.

### Ex vivo function

Eight GST-GUS variants consistently exhibited activity in reactions with X-gluc. The corresponding *gusA* alleles were sequenced, and different mutations at residues 516 and 517 were observed (Table 1). Two mutants include an TAG stop codon at position 516, but were expressed in an amber suppressor strain DH5 $\Delta$ lac(DE3) and thus likely encoded E516. One variant (M516K, Y517E) was isolated twice and was most active when fused to GST. It was first subcloned back into the original vector (pET28a+), thus replacing the N-terminal GST tag with a six-histidine tag.

The GST-M516K/Y517E GUS and his<sub>6</sub>-M516K/Y517E GUS proteins were separately expressed in *E. coli* and purified to homogeneity using either glutathione or immobilized metal affinity chromatography. Each purified protein was separately reacted with 1 mM *p*-nitrophenyl  $\beta$ -D-glucuronide (pNP-gluc) in 50 mM Tris-HCl buffer (pH 7.6), and the formation of the *p*-nitrophenol (pNP) product was

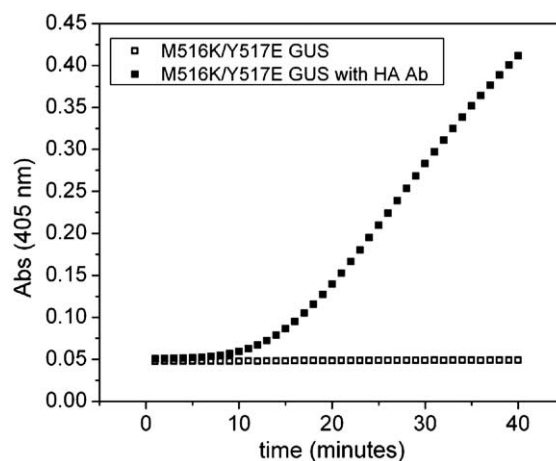


**Figure 2.** Activity assays of his<sub>6</sub>-HA-M516K/Y517E GUS. The purified his<sub>6</sub>-HA-M516K/Y517E GUS protein (50 nM) was reacted with 1 mM pNP-gluc and either 0.5  $\mu$ l of the anti-HA monoclonal antibody (filled squares) or distilled H<sub>2</sub>O (empty squares) in 50 mM Tris, pH 7.6, in a 96-well microplate. The reactions were monitored at 405 nm in a spectrophotometer at 37 °C for 1 h, and the initial activities (Supplemental Table 1) were calculated from the slopes of the lines after the lag phase.

followed at 405 nm in a UV/vis spectrophotometer. The GST-M516K/Y517E GUS (100 nM) consistently showed higher specific activity (8.4 mAbs/min) than equimolar concentrations of his<sub>6</sub>-M516K/Y517E GUS (0.8 mAbs/min). In contrast, the tagged but otherwise wild-type his<sub>6</sub>-GUS and GST-GUS proteins possessed similar specific activity (data not shown).

### Antibody-dependent GUS variant

Although the GST-dependent GUS variant could be used for *in vitro* protein interaction assay, our objective was to design a modular molecular switch that can be activated *in vitro* by an intact antibody. We chose the anti-hemagglutinin (anti-HA) monoclonal antibody as a model analyte to show that oligomerization and activation could be induced by an intermolecular effector. We inserted the DNA sequence encoding the HA epitope (YPYDVPDYA) and a 10-amino-acid spacer immediately upstream of the M516K/Y517E *gusA* gene. The his<sub>6</sub>-HA-M516K/Y517E GUS fusion protein was expressed in *E. coli* and purified to homogeneity by virtue of its his<sub>6</sub> tag; the yield was similar to that of the his<sub>6</sub>-wild type GUS protein (~10 mg/l culture).

Varying quantities of purified his<sub>6</sub>-HA-M516K/Y517E GUS protein (25–200 nM) were reacted with 1 mM pNP-gluc in the presence or absence of saturating (~100 nM) anti-HA monoclonal antibody (typical plot shown in Figure 2). The antibody increased the specific activity of his<sub>6</sub>-HA-M516K/Y517E GUS by a factor of 17 to 300-fold, depending upon the concentration of enzyme (Table 2, Supplemental Table 1). The antibody-dependent increase in activity was inversely proportional to the concentra-

**Table 1.** GST-dependent GUS variants

Clone	Codon 516	Codon 517
Wild-type	Met	Tyr
1-22	Gln	Thr
1-26	Lys	Trp
1-29	Met	Gly
2-10	Stop (Gln) <sup>a</sup>	Tyr
2-17	Lys	Glu
2-24	Lys	Glu
3-7	Stop (Gln) <sup>a</sup>	Tyr
3-18	Ala	Val

<sup>a</sup> The nucleotide sequence for this position was TAG, but all alleles were expressed in *E. coli* amber suppression strain DH5 $\Delta$ lac (DE3), so the protein likely contains a glutamine at this position.

**Table 2.** Activation of his<sub>6</sub>-HA-M516K/Y517E GUS by anti-HA antibody

GUS Concentration	4-Methylumbelliferyl- $\beta$ -D-glucuronide	pNP- $\beta$ -D-glucuronide
10 nM	490 $\pm$ 90	ND
25 nM	400 $\pm$ 100	ND
50 nM	200 $\pm$ 100	300 $\pm$ 170
100 nM	90 $\pm$ 20	360 $\pm$ 180
200 nM	25 $\pm$ 7	100 $\pm$ 70

The values represent the enzyme activity in the presence of the antibody divided by the activity in its absence (Supplemental Table 1).

tion of enzyme, most likely due to a residual tendency toward self-oligomerization. We also used a fluorogenic substrate, 4-methylumbelliferyl- $\beta$ -D-glucuronide (MUG),<sup>20</sup> to improve the sensitivity and observed GUS activation within the assay. We reacted his<sub>6</sub>-HA-M516K/Y517E GUS (10–200 nM) with 1 mM MUG in 50 mM Tris-HCl buffer (pH 7.6) and monitored the release of the fluorescent methylumbelliferone product in a spectrofluorometer. The specific activity of the minimum detectable concentration of his<sub>6</sub>-HA-M516K/Y517E GUS (10 nM) increased ~500-fold upon addition of the anti-HA antibody (Table 2 and Supplementary Table 1). Gel filtration analysis of the his<sub>6</sub>-HA-M516K/Y517E GUS (~116 kDa) and his<sub>6</sub>-HA-wild-type GUS (~235 kDa) suggests the mutant forms an inactive dimer as predicted (Figure 3). Both proteins also eluted at the void volume, suggesting a tendency to aggregate.

As a control, the his<sub>6</sub>-HA-wild-type GUS was expressed, purified, and reacted with the HA antibody. As expected, the antibody had no detectable effect upon enzyme activity (data not shown). To confirm that the antibody specificity of the sensor could be switched, we used site-directed insertion mutagenesis to replace the sequence

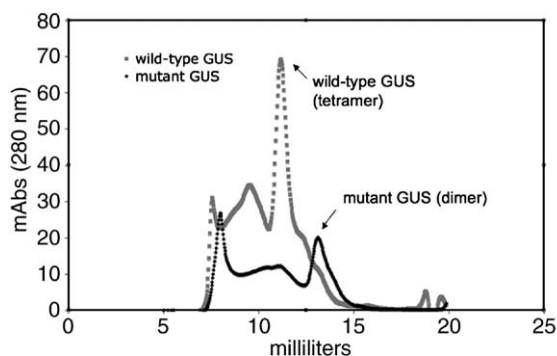


**Figure 3.** Gel filtration of his<sub>6</sub>-HA-wild-type GUS and his<sub>6</sub>-HA-M516K/Y517E GUS. The purified his<sub>6</sub>-HA-M516K/Y517E GUS and his<sub>6</sub>-HA-wild-type GUS proteins were separately run on a Pharmacia Superdex 200 GL 10/300 column equilibrated with 50 mM Tris-HCl (pH 7.6), 150 mM NaCl, and eluted at a flow-rate of 0.5 ml/min. The elution profiles of these proteins were compared with those of molecular mass standards (Bio-Rad). The molecular masses of the mutant and wild-type GUS were determined by extrapolation of the standard curve generated by gel filtration of the Bio-Rad standards.

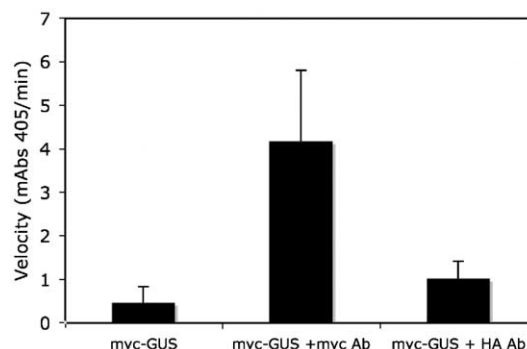


**Figure 4.** Activity assays of his<sub>6</sub>-myc-M516K/Y517E GUS. The purified his<sub>6</sub>-myc-M516K/Y517E GUS protein (100 nM) was reacted with 1 mM pNP-gluc and 2.5  $\mu$ l of distilled H<sub>2</sub>O, the anti-myc monoclonal antibody, or the anti-HA monoclonal antibody in 50 mM Tris, pH 7.6, in a 1-ml cuvette. The reactions were monitored at 405 nm in a spectrophotometer at 37 °C for 1 h, and the initial activities were calculated from the slopes of the lines after the lag phase (Table 2, Supplementary Table 1).

encoding the HA epitope with that encoding the myc tag (EQKLISEEDL). The his<sub>6</sub>-myc-M516K/Y517E GUS protein was expressed, purified, and reacted with 1 mM pNP-gluc in the presence or absence of the anti-myc monoclonal antibody (Figure 4). The antibody increased the specific activity of the his<sub>6</sub>-myc-M516K/Y517E GUS (100 nM) 9-fold. In contrast, the anti-HA monoclonal antibody had no effect, ruling out the possibility that some other factor within the anti-HA antibody sample was nonspecifically activating GUS.

### Kinetic properties of the antibody-dependent GUS variant

The steady-state kinetic parameters ( $k_{cat}$  and  $K_M$ ) of the his<sub>6</sub>-wild-type GUS and antibody-bound his<sub>6</sub>-HA-M516K/Y517E GUS in reactions with pNP-gluc at 37 °C were determined (Table 3). The his<sub>6</sub>-wild-type GUS reaction data readily fit the Michaelis-Menten equation (Figure 5(a)), which suggests the active sites are independent. In contrast, the his<sub>6</sub>-HA-M516K/Y517E GUS reaction data best fit the Hill equation, where  $n$ , the degree of cooperativity, was  $3.7\pm 0.5$  (Figure 5(b)). The data did not fit the Michaelis-Menten equation at all. This result suggests the antibody-bound his<sub>6</sub>-HA-M516K/Y517E GUS binds the pNP-gluc substrate cooperatively. In other words, both the antibody and the substrate are required for maximum enzyme activity. The catalytic

**Table 3.** Steady-state kinetic parameters

Enzyme	Model	$k_{cat}$ (s <sup>-1</sup> )	$K_M$ ( $\mu$ M)	Hill coeff.
Wild-type	Michaelis-Menten	196 $\pm$ 8	340 $\pm$ 30	–
Wild-type	Hill	181 $\pm$ 17	291 $\pm$ 58	1.1 $\pm$ 0.1
Activated mutant	Michaelis-Menten	–	–	–
Activated mutant	Hill	13.7 $\pm$ 1.0	280 $\pm$ 16	3.7 $\pm$ 0.5

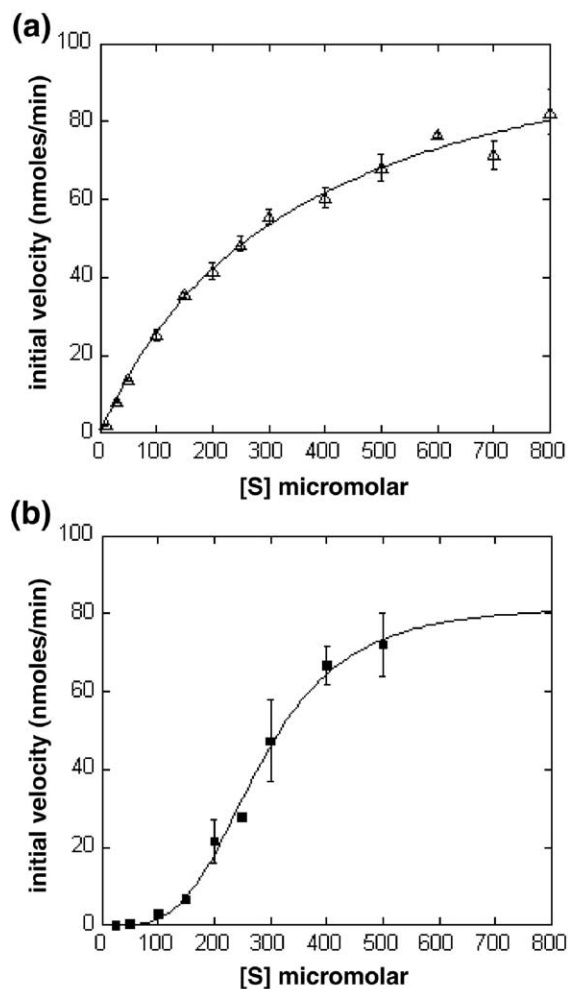


**Figure 5.** Substrate-dependent kinetics of his<sub>6</sub>-wild-type GUS and his<sub>6</sub>-HA-M516K/Y517E GUS. (a) The his<sub>6</sub>-tagged wild-type (empty triangles, 10 nM in 1 ml) or (b) HA-M516K/Y517E GUS bound to an equimolar concentration anti-HA monoclonal antibody (filled squares, 100 nM in 175  $\mu$ l) were separately reacted with 10–800  $\mu$ M pNP-gluc in 50 mM Tris (pH 7.6). The formation of the pNP product was followed in a spectrophotometer. The steady-state kinetic parameters were determined by fitting the initial velocity values to the Michaelis–Menten and Hill equations (Table 3).

efficiency ( $k_{\text{cat}}/K_M$ ) of the activated mutant is  $\sim 9\%$  of the wild-type value, demonstrating that GUS-based biosensors are potentially active enough for rapid point-of-care diagnostic assays.

## Discussion

We used site-saturation mutagenesis in conjunction with negative and positive histochemical screens to generate a GUS mutant that can be activated either by fusion to the dimeric GST protein or by noncovalent interaction with anti-HA (or anti-*myc*) monoclonal antibodies. The mutagenesis and screening strategies were designed to identify mutants that form inactive dimers, but retain a latent

capacity to form active tetramers. It remains formally possible that the activation occurs through an allosteric mechanism,<sup>10</sup> but several lines of evidence favor the induced oligomerization hypothesis. Gel filtration analysis showed that his<sub>6</sub>-M516K/Y517E GUS is mostly dimeric, and his<sub>6</sub>-wild-type GUS is mostly tetrameric (Figure 3).

The correlation between enzyme activity and tetramerization is easy to rationalize. Residues R562 and E557, which are thought to participate in substrate recognition,<sup>21</sup> are in the short subunit interface (blue and green balls in Figure 1). We propose that the nonconservative M516K and Y517E mutations disrupt the association of subunits across the short interface. The energetic cost of burying these two charged residues in the mostly hydrophobic interface (plus the usual entropic cost of oligomerization) exceeds the remaining binding energy. The active sites within the dissociated mutant dimers likely adopt an alternative conformation that is not conducive for catalysis. The binding energy of the bivalent monoclonal antibody helps overcome the energetic cost of burying the charged K516 and E517 residues, thereby shifting the equilibrium toward the tetramer.

The antibody-bound M516K/Y517E GUS displays two unusual kinetic traits consistent with the induced oligomerization mechanism. First, the antibody/enzyme complex exhibits very cooperative substrate binding; the Hill coefficient is similar to that of hemoglobin (Table 3; Figure 5(b)). Previous workers similarly showed mutations in the subunit interface of glutathione reductase,<sup>22</sup> and aspartate receptor<sup>23</sup> can produce mutants that bind their substrate cooperatively. Second, a pronounced  $\sim 10$ -min lag occurs before the enzyme-catalyzed hydrolysis of pNP-gluc enters the steady state (Figure 2); preincubation of our sensors with antibody does not affect the lag (data not shown). We propose that the mutant active site begins in a nonproductive conformation and that antibody binding is not sufficient to stabilize the optimal configuration of the dimers for catalysis. Substrate binding is cooperative because it favors the reconfiguration of the neighboring active-site and the proper assembly of tetramer with productively folded active sites. Slow conformational changes on this time scale were previously observed in mutant proteins.<sup>24</sup>

The sensitivity of a biosensor is defined by the dependence of its activity upon the concentration of analyte. We estimate that  $\sim 100$  nM of an anti-HA antibody was required for maximum activation of 10 nM his<sub>6</sub>-HA-M516K/Y517E GUS. We do not know why a molar excess of antibody is required, but can propose three non-exclusive explanations. First, the commercially available antibody we used might not bind the epitope tightly ( $K_D > 10$  nM). A different anti-HA monoclonal antibody (17/9) exhibited an  $IC_{50}$  of  $3.5 \times 10^{-7}$  M in reactions with the HA tag peptide, and an  $IC_{50}$  of  $1 \times 10^{-8}$  M with a longer peptide that includes the HA tag.<sup>25</sup> Different antibodies, however, exhibit different binding affinities.

Second, the his<sub>6</sub>-HA-M516K/Y517E GUS protein might not display the HA epitope efficiently. The

structure of the wild-type *E. coli* protein has not been solved. Our mutagenesis strategy was guided by a homology model based upon the human GUS structure,<sup>13</sup> but the sequences of the N and C termini of these homologues are highly divergent. The bilateral symmetry of the GUS tetramer makes it possible to display epitopes on geometrically permissive surface loops. Crystal structures of intact IgG antibodies<sup>26</sup> suggest antigens up to 70 Å apart could still be bound by a single bivalent antibody molecule. Third, the M516K/Y517E mutation combination was selected for responsiveness (i.e., ~500-fold activation by antibody) rather than for sensitivity. Mutations in the subunit interface that are less deleterious would likely create more sensitive (and less responsive) sensors. The optimization of these parameters should enable molecular switches suitable for the detection of antibodies (and possibly other multimeric protein analytes) within clinical samples.

Our design strategy could be used to convert multimeric proteins other than GUS into molecular switches. Most reporter proteins, including  $\beta$ -galactosidase, alkaline phosphatase, and glucose oxidase, and ~35% of all intracellular proteins<sup>27</sup> require oligomerization for activity. Previous workers mutated residues in the subunit interfaces of alkaline phosphatase<sup>28</sup> and GST.<sup>29</sup> In both studies, the size and charge of the substituted amino acid caused shifts in the monomer-dimer equilibria of these proteins. We identified several different mutation combinations that favored the formation inactive GUS dimers (Table 1). The most GST-dependent variant (M617K, Y157E) contained charged residues that are energetically costly to bury. Site-directed mutagenesis could be used to introduce analogous amino acid replacements into almost any oligomeric enzyme.

The current standard in immunological assays is ELISA. In this labor-intensive technique, antibodies that recognize pathogen markers are adsorbed to 96-well plates. Samples are reacted with the plate-bound antibodies; unbound molecules are washed away. The antibody-antigen complexes are reacted with a second detection antibody that recognizes a separate epitope of the antigen. The second antibody is usually conjugated to a reporter enzyme. The complexes are washed to remove unbound reporter enzyme and then reacted with a colorimetric substrate. Our sensor reacts with an antibody and a fluorescent substrate in solution without any washing steps and, therefore, represents a simpler approach to molecular detection. The development of switches with different activities (outputs) could someday enable multiplex serological assays.

## Materials and Methods

### Materials

Expression vectors pET28a+ and pET42a+ were from Novagen (Madison, WI, USA). *E. coli* strain BL21 (DE3) Gold/pLysS was from Stratagene (La Jolla, CA, USA); DH5 $\Delta$ lac(DE3) was described previously.<sup>21</sup> The oligonu-

cleotides were synthesized by IDT (Coralville, IA, USA); the pNP-gluc and MUG were from Sigma-Aldrich, and the X-gluc was from Gold Biotechnology (both St. Louis, MO, USA). The mouse monoclonal anti-HA and anti-myc antibodies were from Covance (Princeton, NJ, USA). The BigDye 3.1 DNA sequencing and GeneAmp XL Long PCR kits were from Applied Biosystems (Foster City, CA, USA).

### Site-saturation mutagenesis and screening

The *gusA* codons encoding amino acids 516 and 517 (within expression vector his<sub>6</sub>-*gusA*-pET28a+) were randomized by whole plasmid PCR<sup>30</sup> using the following 5' phosphorylated degenerate primers: 5'-GGGCTGCACTC-CANNKNNKACCGACATGTGGA-3' and 5'-GGCTAAC-GTATCCACGCCGTATTCGGTG-3'. The library was then generated by the purification, self-ligation, and transformation of strain DH5 $\Delta$ lac(DE3) as previously described.<sup>17</sup> The his<sub>6</sub>-*gusA* clones exhibiting no GUS activity were subcloned into expression vector pET42a+(immediately downstream of the GST gene) using the restriction enzymes NcoI and HindIII.

### Insertion of epitope tags

The most GST-dependent *gusA* allele (M516K/Y517E) was subcloned back into pET28a+(immediately downstream of the his<sub>6</sub> tag sequence) using restriction endonucleases NcoI and HindIII. We previously generated the HA epitope within the unstructured region of p53,<sup>31</sup> DNA sequences from this construct encoding the HA epitope and a 10-amino-acid p53 linker to the 5' end of M516K/Y517E *gusA* (his<sub>6</sub>-HA-linker-*gusA*) through the following overlap PCR procedure. The HA tag was PCR amplified from HA-p53-delta68-pET28a+<sup>31</sup> using primers 5'-TTGG-GTTTCTACAGGACGTAACATATGTCTGGGAGCTT-CATCTGGACCTGGG-3' (p53rev196/5'*gusA*) and 5'-GAGTCTCGATCCCGCGAAATTAATACGA-3' (5'*pET*). The 5' end of the his<sub>6</sub>-M516K/Y517E *gusA*-pET28a+ was amplified with 5'-CCCAGGTCCAGATGAAGCTCCCA-GACATATGTTACGTCCTGTAGAAACCCCAA (5'*gusA*/p53rev196) and 5'-GCTCAGCGGTGGCAGCCAGCCAACTC-3' (GC 3'*pET*). Each PCR product was purified with a Qiagen silica spin column as directed by the manufacturer. The two purified PCR products (50 ng each) were recombined and PCR amplified in a third PCR using the 5'*pET* GC 3'*pET* primers. The full-length his<sub>6</sub>-HA-M516K/Y517E *gusA* PCR product was purified with a Qiagen silica spin column and cloned back into the his<sub>6</sub>-M516K/Y517E *gusA*-pET28a+ plasmid using restriction enzymes MscI and NcoI. The resulting clones were sequenced with the 5' *pET* primer to confirm the presence of the HA epitope tag. After this stage of cloning, there remained 45 amino acids between the his<sub>6</sub> tag and the HA epitope tag.

The upstream region of p53 was removed through whole plasmid PCR with the phosphorylated primers -5'-TATCCGATGATGTGCCGATTATGCG-3' (p53HA*gusA*) and 5'-CATATGGCTGCCGCGCGGCCACCA-3' (p53HA*gusA*rev). The resulting his<sub>6</sub>-HA-linker-*gusA* construct was sequenced in its entirety to confirm that no undesired random mutations were introduced during the PCR amplification steps. The myc tag was inserted by using his<sub>6</sub>-HA-M516K/Y517E *gusA*-pET28a+ as a template with the primers -5'AATCAGTTTCTGTTCCATATGGCTGC-CGCGCGCACCCAG-3' (myc*gusA*rev) -5'AGCGAAGAA-GATCTGACTGAAGACCCAGGTCCAGATGAAGC-3' (myc*gusA*out) in a whole plasmid PCR as described above.

DNA sequencing showed the resulting product encoded the *myc* epitope instead of the HA epitope.

### Sequencing

The *gusA* alleles were sequenced using the Applied Biosystems BigDye protocol at the Center for Fundamental and Applied Molecular Evolution (Emory University). The 3' end of every *gusA* allele in this paper was sequenced using the primer GC 3'pET. his<sub>6</sub>-M516K/Y517E *gusA*-pET28a+, GST-M516K/Y517E *gusA*-pET42a+, and his<sub>6</sub>-HA-M516K/Y517E *gusA*-pET28a+ were sequenced in their entirety, using the following additional primers: 5' pET, 5'-GCCATTGAAGCCGATGTCACGCCG-3' (*gusA* 360), 5'-GGACTTTGCAAGTGGTGAATCCGCAC-3' (*gusA* 720), and 5'-CTGCTGCTGTCGGCTTAAACCTCT-CT-3' (*gusA* 1080).

### Protein purification—GST and IMAC

The his<sub>6</sub>-tagged GUS variants were chemically transformed into BL21(DE3)Gold/pLysS. The variants were expressed at room temperature overnight and lysed by sonication after suspension in 50 mM Tris, pH 7.6, and 0.5 M NaCl. They were then purified as described.<sup>17</sup> The GST-tagged GUS variants were purified from the DH5 $\Delta$ lac(DE3) strain according to the manufacturer's instructions (Novagen). All proteins used in this study were >95% pure as judged by SDS-PAGE. The concentrations of each purified protein were quantified using the Bradford protein assay (Bio-Rad, Hercules, CA, USA). Molar concentrations were based on the number of GUS active-sites subunit molecular weight=682,000.

### Enzyme assays

The purified GUS proteins were diluted to 25 to 200 nM and reacted with 1 mM pNP-gluc and either 0.5  $\mu$ l of the anti-HA monoclonal antibody, anti-*myc* antibody, or distilled H<sub>2</sub>O in 50 mM Tris, pH 7.6, in a 96-well microplate (Nunc). Based upon estimates by the manufacturer (Covance), we calculate that the final concentration of antibody (molecular mass=150,000) is ~100 nM. The reactions were monitored in a Thermo LabSystems Multiskan microplate spectrophotometer at 37 °C for 1 h, and the initial activities were calculated from the slopes of the lines after the lag phase. For the fluorescent assays, 1 mM of MUG was added to 10–200 nM of protein in 50 mM Tris, pH 7.6. The reaction was monitored in a fluorometer at 37 °C for 30 min or until the substrate was depleted.

To determine the steady-state kinetic parameters, his<sub>6</sub>-wild-type GUS (10 nM) was reacted with 10–800  $\mu$ M pNP-gluc in 50 mM Tris (pH 7.6); all reactions were conducted in triplicate in a 1 ml (1-cm path-length) polystyrene cuvette (Thermo Fisher Scientific). The formation of the pNP product at 37 °C was followed in a Shimadzu UV-1601 spectrophotometer. The absorption extinction coefficient of pNP at 405 nm under these conditions is 16.64 mM<sup>-1</sup> cm<sup>-1</sup>. The his<sub>6</sub>-HA-M516K/Y517E GUS (100 nM) was mixed with approximately equimolar anti-HA antibody and 10–500  $\mu$ M pNP-gluc in a microfuge tube (again, in triplicate). The reactants (175  $\mu$ l) were transferred to a small quartz cuvette (0.3 cm $\times$ 0.3 cm $\times$ 27 mm), and product formation at 37 °C was monitored in the spectrophotometer. The initial velocity values (excluding the lag exhibited by the antibody-bound his<sub>6</sub>-HA-M516K/Y517E

GUS and taking into account the smaller volume and cuvette path-length) were fit to the Michaelis–Menten and Hill equations

$$v_i = \frac{V_{\max} * [S]^n}{K_M^n + [S]^n}$$

(where  $n$  is the Hill coefficient, a measure of cooperativity) by the nonlinear least-squares algorithm of Kaleidagraph 3.0.5 (Adelbeck Software, Reading, PA, USA).

### Gel filtration

The purified his<sub>6</sub>-M516K/Y517E GUS and his<sub>6</sub>-wild-type GUS proteins were separately run on a Pharmacia Superdex 200 GL 10/300 column equilibrated with 50 mM Tris-HCl (pH 7.6), 150 mM NaCl, and eluted at a flow rate of 0.5 ml/min. The elution profiles of these proteins were compared to those of molecular mass standards (Bio-Rad). The molecular mass of the mutant and wild-type GUS was determined by extrapolation of the standard curve generated by gel filtration of the Bio-Rad standards.

### Acknowledgements

We thank Dr. Monica Gerth and Dr. Stefan Lutz for their assistance with the gel filtration experiment, as well as Jeff Boyd for his advice on data analysis. Both MG and IM were supported by a grant from NIH/NIGMS (1 R01 GM074264-01).

### Supplementary Data

Supplementary data associated with this article can be found, in the online version, at [doi:10.1016/j.jmb.2007.03.076](https://doi.org/10.1016/j.jmb.2007.03.076)

### References

1. von Lode, P. (2005). Point-of-care immunotesting: approaching the analytical performance of central laboratory methods. *Clin. Biochem.* **38**, 591–606.
2. Frankel, A. E., Powell, B. L., Duesbery, N. S., Vande Woude, G. F. & Leppla, S. H. (2002). Anthrax fusion protein therapy of cancer. *Curr. Protein Peptide Sci.* **3**, 399–407.
3. Bagshawe, K. D. (2006). Antibody-directed enzyme prodrug therapy (ADEPT) for cancer. *Expert Rev. Anticancer Ther.* **6**, 1421–1431.
4. Bhattacharyya, R. P., Remenyi, A., Yeh, B. J. & Lim, W. A. (2006). Domains, motifs, and scaffolds: the role of modular interactions in the evolution and wiring of cell signaling circuits. *Annu. Rev. Biochem.* **75**, 655–680.
5. Swain, J. F. & Gierasch, L. M. (2006). The changing landscape of protein allostery. *Curr. Opin. Struct. Biol.* **16**, 102–108.
6. Feliu, J. X. & Villaverde, A. (1998). Engineering of solvent-exposed loops in *Escherichia coli* beta-galactosidase. *FEBS Letters*, **434**, 23–27.
7. Brennan, C. A., Christianson, K., La Fleur, M. A. & Mandecki, W. (1995). A molecular sensor system based on genetically engineered alkaline phosphatase. *Proc. Natl Acad. Sci. USA*, **92**, 5783–5787.

8. Legendre, D., Soumillion, P. & Fastrez, J. (1999). Engineering a regulatable enzyme for homogeneous immunoassays. *Nature Biotechnol.* **17**, 67–72.
9. Ferrer-Miralles, N., Feliu, J. X. & Villaverde, A. (2000). Molecular mechanisms for antibody-mediated modulation of peptide-displaying enzyme sensors. *Biochem. Biophys. Res. Commun.* **275**, 360–364.
10. Villaverde, A. (2003). Allosteric enzymes as biosensors for molecular diagnosis. *FEBS Letters*, **554**, 169–172.
11. Guntas, G. & Ostermeier, M. (2004). Creation of an allosteric enzyme by domain insertion. *J. Mol. Biol.* **336**, 263–273.
12. Guntas, G., Mansell, T. J., Kim, J. R. & Ostermeier, M. (2005). Directed evolution of protein switches and their application to the creation of ligand-binding proteins. *Proc. Natl Acad. Sci. USA*, **102**, 11224–11229.
13. Jain, S., Drendel, W. B., Chen, Z. W., Mathews, F. S., Sly, W. S. & Grubb, J. H. (1996). Structure of human beta-glucuronidase reveals candidate lysosomal targeting and active-site motifs. *Nature Struct. Biol.* **3**, 375–381.
14. Haldeman, M. T., Xia, G., Kasperek, E. M. & Pickart, C. M. (1997). Structure and function of ubiquitin conjugating enzyme E2-25K: the tail is a core-dependent activity element. *Biochemistry*, **36**, 10526–10537.
15. Niedziela-Majka, A., Rymarczyk, G., Kochman, M. & Ozyhar, A. (1998). GST-induced dimerization of DNA-binding domains alters characteristics of their interaction with DNA. *Protein Expr. Purif.* **14**, 208–220.
16. Flores, H. & Ellington, A. D. (2002). Increasing the thermal stability of an oligomeric protein, beta-glucuronidase. *J. Mol. Biol.* **315**, 325–337.
17. Geddie, M. L. & Matsumura, I. (2004). Rapid evolution of beta-glucuronidase specificity by saturation mutagenesis of an active site loop. *J. Biol. Chem.* **279**, 26462–26468.
18. Cheng, S., Fockler, C., Barnes, W. M. & Higuchi, R. (1994). Effective amplification of long targets from cloned inserts and human genomic DNA. *Proc. Natl Acad. Sci. USA*, **91**, 5695–5699.
19. Lim, K., Ho, J. X., Keeling, K., Gilliland, G. L., Ji, X., Ruker, F. & Carter, D. C. (1994). Three-dimensional structure of *Schistosoma japonicum* glutathione S-transferase fused with a six-amino acid conserved neutralizing epitope of gp41 from HIV. *Protein Sci.* **3**, 2233–2244.
20. Naleway, J. J. (1992). Histochemical, spectrophotometric, and fluorometric GUS substrates. In *GUS Protocols: Using the GUS Gene as a Reporter of Gene Expression* (Gallagher, S. R., ed), pp. 61–76, Academic Press, New York.
21. Matsumura, I. & Ellington, A. D. (2001). In vitro evolution of beta-glucuronidase into a beta-galactosidase proceeds through non-specific intermediates. *J. Mol. Biol.* **305**, 331–339.
22. Scrutton, N. S., Deonarain, M. P., Berry, A. & Perham, R. N. (1992). Cooperativity induced by a single mutation at the subunit interface of a dimeric enzyme: glutathione reductase. *Science*, **258**, 1140–1143.
23. Kolodziej, A. F., Tan, T. & Koshland, D. E., Jr (1996). Producing positive, negative, and no cooperativity by mutations at a single residue located at the subunit interface in the aspartate receptor of *Salmonella typhimurium*. *Biochemistry*, **35**, 14782–14792.
24. Onuffer, J. J. & Kirsch, J. F. (1994). Characterization of the apparent negative co-operativity induced in *Escherichia coli* aspartate aminotransferase by the replacement of Asp222 with alanine. Evidence for an extremely slow conformational change. *Protein Eng.* **7**, 413–424.
25. Schulze-Gahmen, U., Rini, J. M., Arevalo, J., Stura, E. A., Kenten, J. H. & Wilson, I. A. (1988). Preliminary crystallographic data, primary sequence, and binding data for an anti-peptide Fab and its complex with a synthetic peptide from influenza virus hemagglutinin. *J. Biol. Chem.* **263**, 17100–17105.
26. Saphire, E. O., Parren, P. W., Pantophlet, R., Zwick, M. B., Morris, G. M. & Rudd, P. M. (2001). Crystal structure of a neutralizing human IgG against HIV-1: a template for vaccine design. *Science*, **293**, 1155–1159.
27. Ali, M. H. & Imperiali, B. (2005). Protein oligomerization: how and why. *Bioorg. Med. Chem.* **13**, 5013–5020.
28. Boulanger, R. R., Jr & Kantrowitz, E. R. (2003). Characterization of a monomeric *Escherichia coli* alkaline phosphatase formed upon a single amino acid substitution. *J. Biol. Chem.* **278**, 23497–23501.
29. Vargo, M. A., Nguyen, L. & Colman, R. F. (2004). Subunit interface residues of glutathione S-transferase A1-1 that are important in the monomer-dimer equilibrium. *Biochemistry*, **43**, 3327–3335.
30. Eisinger, D. P. & Trumppower, B. L. (1997). Long-inverse PCR to generate regional peptide libraries by codon mutagenesis. *Biotechniques*, **22**, 250–252, 254.
31. Geddie, M. L., O'Loughlin, T. L., Woods, K. K. & Matsumura, I. (2005). Rational design of p53, an intrinsically unstructured protein, for the fabrication of novel molecular sensors. *J. Biol. Chem.* **280**, 35641–35646.

Edited by J. Karn

(Received 13 November 2006; received in revised form 19 March 2007; accepted 27 March 2007)